

electrolytic capacitors. Additionally, they exhibit rapid charge–discharge capability and a much longer cycle life than traditional rechargeable batteries. Consequently, the development of efficient, low-cost and renewable electrode materials for supercapacitors has become a necessity for developing societies [1].

Activated carbon derived from biomass has emerged as a highly promising material for electrochemical applications owing to its environmentally benign and sustainable nature. Plant-based activated carbons are increasingly recognized as multifunctional alternatives due to their abundant availability, low cost, and renewable origin. These materials have found wide-ranging applications in wastewater treatment, air and water purification, food processing, and energy storage devices, particularly supercapacitors, where their high surface area and tunable porosity offer significant performance advantages. [2,3].

The production of biomass-derived activated carbon (BDAC) typically involves two key steps: carbonization and activation. Carbonization converts biomass into char, while activation using activating agents such as KOH, NaOH, or $ZnCl_2$ enhancing porosity and surface area [4,5]. The resulting activated carbon materials exhibit high specific surface area, tunable pore size distribution, and abundant surface functional groups, making them highly effective for photocatalytic dye degradation and charge storage applications.

In the present work, activated carbon derived from betel leaf is investigated to assess its suitability for supercapacitor applications. The surface characteristics, crystalline structure, particle morphology, and elemental composition of the synthesized activated carbon are systematically analyzed using X-ray diffraction (XRD), field-emission scanning electron microscopy (FESEM), energy-dispersive X-ray analysis (EDAX), and UV–visible spectroscopy. Further, electrochemical studies are conducted to evaluate its performance as an electrode material for supercapacitors.

2 Design

2.1 Materials

Potassium hydroxide pellets ($\geq 99\%$) from Merck, India and fresh betel leaves were procured from local market.

2.2. Green synthesis of activated carbon

Fresh betel leaves were thoroughly washed, dried, and ground into a fine powder. The resulting powder was initially carbonized at 300 °C using a muffle furnace. Further the 0.5 g of potassium hydroxide (KOH) and 2 g of the carbonized powder were mixed, and the mixture was well grounded using mortar to guarantee even dispersion. This mixture was then subjected to thermal treatment at 400 °C for 1 hour.



Scheme 1 Synthesis of activated carbon

2.3. Characterization

The UV-Vis absorption measurements were conducted in visible range using spectrophotometer (Ocean Optics Maya 2000). The high-resolution surface image of the sample was obtained from field emission scanning electron microscope (FESEM, Carl Zeiss). Elemental composition was obtained using Energy-dispersive X-ray analysis (EDAX) Bruker model. The electrochemical measurements were conducted using three electrode system with Ag/AgCl as reference electrode and Platinum as counter electrode using Admiral Squid stat Plus.

3 Discussion

The XRD analysis of the synthesized sample shown in Fig.1 with characteristic carbon peaks at 26.08 and 40.9 degrees corresponds to graphitic carbon (JCPDS-00-056-0159) in agreement with previous data [6]. The peak at 30.08 degrees corresponds to the presence of potassium.

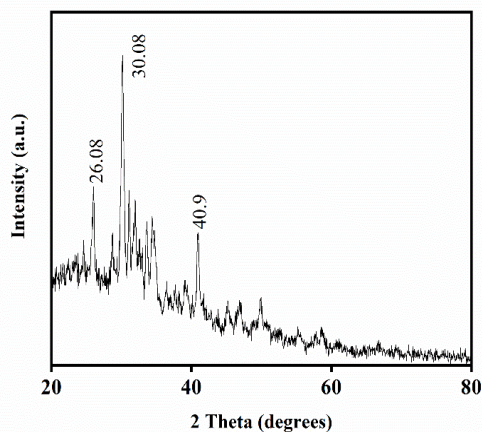


Fig.1 XRD analysis of the activated carbon sample

The crystallite size is obtained from the Scherrer formula

$$\theta = \frac{0.89\lambda}{\beta \cos\theta}$$

where θ represents the Bragg angle (in degrees), β the line broadening at half the maximum intensity (FWHM), and λ the X-ray wavelength. The crystallite size was found to be 25.85 nm.

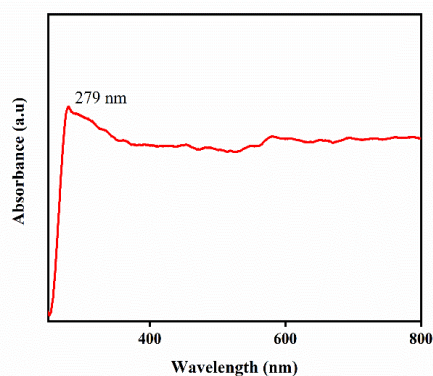


Fig.2 UV analysis of the sample

The UV peak at 279 nm as shown in Fig.2 corresponds the typical carbon peak as per previous reports [7]. The surface morphology of the activated carbon derived from betel leaf was examined using FESEM is shown in Fig.3. The SEM images revealed the presence of irregularly shaped particles with a porous structure. These pores are most likely developed as a result of the leaf powder's thermal decomposition during carbonization [8] and also due to the chemical activation by KOH, which facilitates the removal of volatile components and enhances pore formation. The porous morphology is beneficial for applications such as adsorption and energy storage, as it provides a high surface area for interaction with ions or molecules.

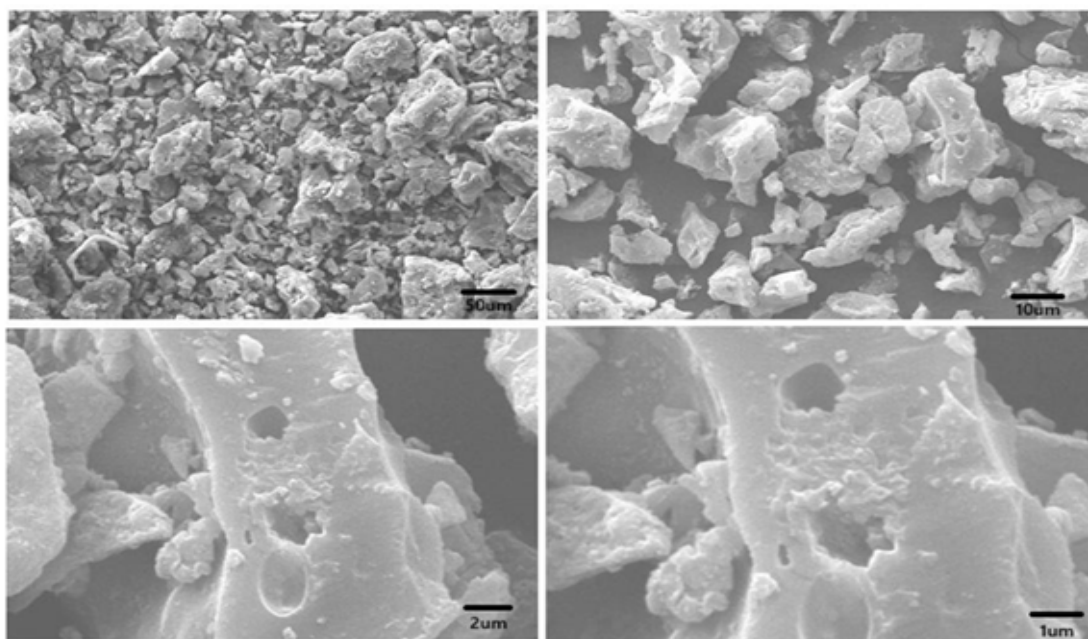


Fig.3 SEM images with different magnifications

Fig.4 shows the elemental composition of the activated carbon derived from betel leaf analyzed using EDAX. The spectrum revealed a predominant presence of carbon (64.04 wt%), confirming the carbon-rich nature of the material which is consistent with previous reports [9]. A

significant amount of oxygen (21.89 wt%) was also detected, indicating various types of oxygen containing functional groups which are beneficial for enhancing surface reactivity and adsorption properties. Notably, potassium (9.84 wt%) was observed, attributed to residual K from the KOH activation process, suggesting partial retention of the activating agent in the carbon matrix. The overall elemental profile supports the successful synthesis of activated carbon suitable for adsorption and electrochemical applications. The amount of carbon in the can be further enhanced by increasing the carbonization temperature at inert conditions.

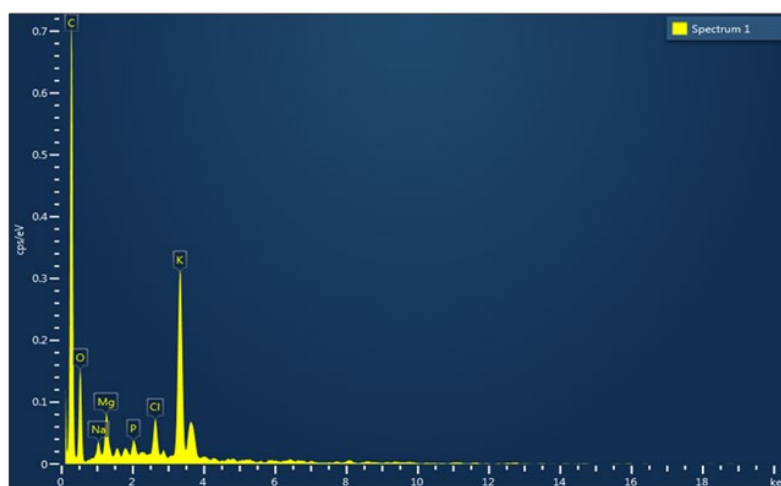


Fig.4 EDAX analysis of the synthesized sample

Cyclic Voltammetry (CV) analysis was used to examine the sample's supercapacitor behaviour with 1 M Na_2SO_4 electrolyte in a conventional three-electrode configuration in the potential window ranging from -0.8V to 0.8 V as shown in Fig. 5(a). The nearly rectangular voltammograms acquired for scan rates between 10 and 100 mV/s demonstrate the typical capacitive electrode behaviour of the sample.

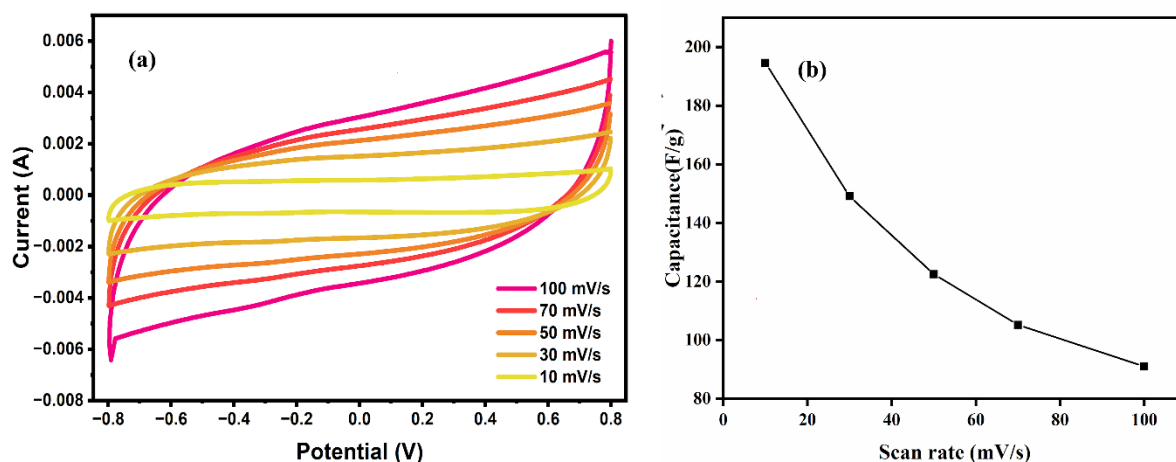


Fig.5 (a) CV curves of the sample (b) Specific capacitance values at different scan rates

The specific capacitance was obtained using the equation from discharge curve

$$C_{sp} = \frac{A}{2(k \times m \times \Delta V)}$$

where the discharge curve's area is denoted by A , the electrode material's mass by m , the scan rate by k , and the applied potential difference by ΔV .

For scan speeds 10, 30, 50, 70, and 100 mV/s, the corresponding specific capacitance values are 194.6, 149.1, 122.5, 105.2, and 91.07 F/g (Fig. 5b). The specific capacitance is found to decrease with increasing scan rate because, in contrast to small scan rates, greater scan rates reduce ion diffusion and storage because of lack of time [10,11].

4 Conclusion

In this investigation, we synthesized cost-effective and environmentally sustainable biomass-derived activated carbon with chemical activation via KOH. The sample synthesized was characterized by XRD, UV, SEM and EDAX measurements. The SEM analysis showed that the material exhibited porous structure favorable for adsorption and ion transport. The cyclic

voltammetry studies showed maximum specific capacitance of 194.6 F/g for a scan rate of 10 mV/s indicating good capacitive behaviour. Overall, biomass-derived activated carbon presents itself as a sustainable, cost-effective, and high-performance material suitable for energy storage devices.

References

1. Zhaoxiang, Qi., & Koenig G. M, Jr. (2017). *Review Article: Flow battery systems with solid electroactive materials*, Journal of Vacuum Science and Technology B, 35(4), 040801.
2. Krishnan, S. G., Harilal, M., Pal, B., Misnon, I. I., Karuppiah, C., Yang, C. C., & Jose, R. (2017). *Improving the symmetry of asymmetric supercapacitors using battery-type positive electrodes and activated carbon negative electrodes by mass and charge balance*. Journal of Electroanalytical Chemistry, 805, 126-132.
3. Heidarinejad, Z., Dehghani, M. H., Heidari, M., Javedan, G., Ali, I., & Sillanpää, M. (2020). *Methods for preparation and activation of activated carbon: a review*. Environmental Chemistry Letters, 18, 393-415.
4. Nita, C., Zhang, B., Dentzer, J., & Ghimbeu, C. M. (2021). *Hard carbon derived from coconut shells, walnut shells, and corn silk biomass waste exhibiting high capacity for Na-ion batteries*. Journal of Energy Chemistry, 58, 207-218.
5. Hegde, S. S., & Bhat, B. R. (2024). *Sustainable energy storage: Mangifera indica leaf waste-derived activated carbon for long-life, high-performance supercapacitors*. RSC advances, 14(12), 8028-8038.
6. Yetri, Y., Afza, V. Y. Y., Ganumba, O., & Sunitra, E. (2023, August). *Effect of Electrolyte Concentration on Characteristics of Activated Carbon of Cocoa Peel*. In IOP Conference Series: Earth and Environmental Science (Vol. 1228, No. 1, p. 012042). IOP Publishing.
7. Uran, S., Alhani, A., & Silva, C. (2017). *Study of ultraviolet-visible light absorbance of exfoliated graphite forms*. AIP Advances, 7(3).

8. Moheb, M., El-Wakil, A. M., & Awad, F. S. (2025). *Highly porous activated carbon derived from the papaya plant (stems and leaves) for superior adsorption of alizarin red s and methylene blue dyes from wastewater*. RSC advances, 15(1), 674-687.
9. Hussain, O. A., Hathout, A. S., Abdel-Mobdy, Y. E., Rashed, M. M., Rahim, E. A., & Fouzy, A. S. M. (2023). *Preparation and characterization of activated carbon from agricultural wastes and their ability to remove chlorpyrifos from water*. Toxicology Reports, 10, 146-154.
10. Elgrishi, N., Rountree, K. J., McCarthy, B. D., Rountree, E. S., Eisenhart, T. T., & Dempsey, J. L. (2018). *A practical beginner's guide to cyclic voltammetry*. Journal of chemical education, 95(2), 197-206.
11. Ahmad, A., Gondal, M. A., Hassan, M., Iqbal, R., Ullah, S., Alzahrani, A. S., & Melhi, S. (2023). *Preparation and characterization of physically activated carbon and its energetic application for all-solid-state supercapacitors: a case study*. ACS omega, 8(24), 21653-21663.